Climatic Change (2011) 104:575–597
DOI 10.1007/s10584-009-9790-0

Global warming and hurricanes: the potential impact of hurricane intensification and sea level rise on coastal flooding

Mir Emad Mousavi · Jennifer L. Irish · Ashley E. Frey · Francisco Olivera · Billy L. Edge

Received: 26 January 2009 / Accepted: 11 December 2009 / Published online: 12 January 2010

Abstract Tens of millions of people around the world are already exposed to coastal flooding from tropical cyclones. Global warming has the potential to increase hurricane flooding, both by hurricane intensification and by sea level rise. In this paper, the impact of hurricane intensification and sea level rise are evaluated using hydrodynamic surge models and by considering the future climate projections of the Intergovernmental Panel on Climate Change. For the Corpus Christi, Texas, United States study region, mean projections indicate hurricane flood elevation (meteorologically generated storm surge plus sea level rise) will, on average, rise by 0.3 m by the 2030s and by 0.8 m by the 2080s. For catastrophic-type hurricane surge events, flood elevations are projected to rise by as much as 0.5 m and 1.8 m by the 2030s and 2080s, respectively.

Abbreviations

IPCC	Intergovernmental Panel on Climate Change
MSL	Mean sea level
NOAA	National Oceanic and Atmospheric Administration
SLR	Sea level rise
SRF	Surge response function
SST	Sea surface temperature

1 Introduction

Hurricanes and other tropical cyclones pose one of the most significant natural threats to coastal communities worldwide. High winds and surges, and, in inland regions, rainfall, can cause significant damage. Over the last 5 years, the USA has

M. E. Mousavi · J. L. Irish (✉) · A. E. Frey · F. Olivera · B. L. Edge
Zachry Department of Civil Engineering, Texas A&M University,
College Station, TX 77843-3136, USA
e-mail: jirish@civil.tamu.edu

seen record numbers of hurricane landfalls and has experienced the devastating effects of some of the highest hurricane surges on record, including those of Hurricanes Katrina, Rita, and Ike (e.g., Travis 2005; Irish et al. 2008a; Federal Emergency Management Agency 2008). Recent climatic research indicates that, in response to global warming, hurricanes may intensify and sea level rise (SLR) may accelerate (Intergovernmental Panel on Climate Change [IPCC] 2007). The coupled effect of these two phenomena will lead to increased hurricane flood risk at the coast, thereby potentially increasing coastal flooding during hurricane events.

Here we investigate the potential impact of global warming on hurricane flood levels by considering the coupled influence of projected hurricane intensification and accelerated SLR at Corpus Christi, Texas, USA, in the Gulf of Mexico. Our analysis shows that if future global warming projections are realized, coastal flood levels have the potential to rise significantly over the next 80 years, making coastal communities progressively more vulnerable to hurricane damage.

In the following sections, we discuss the influencing climatic factors leading to potential escalation in hurricane flooding, introduce the numerical simulation approach, and present our results and conclusions regarding future hurricane flooding into the 2080s.

2 Background

Future climate variability has the capacity to alter hurricane flooding through decadal and long-term trends in hurricane frequency and hurricane intensity as well as in SLR. In this paper, we will focus on long-term projections of global warming; although we recognize that shorter-scale decadal cycles, such as the El Niño-Southern Oscillation (ENSO) and astronomical tidal influences, also change hurricane activity and mean water levels.

By considering a suite of future climate scenarios, the IPCC (2007) projected global surface temperature increases between 1.1 and 6.4°C over the next century. To span the range of potential future global warming scenarios, we consider here three of the IPCC future climate scenarios: (1) B1, a global mean temperature rise estimate for a low rate of greenhouse gas emissions and hence global warming; (2) A1B, a mid-range emissions scenario; and (3) A1FI, the highest emissions scenario published by the IPCC (Nakićenovic et al. 2000). Each of these future warming scenarios can be used to evaluate the potential impact of global warming on hurricane flooding by estimating the expected amount of hurricane intensification and SLR for each climate scenario.

2.1 Potential influence of global warming on hurricane intensity

Recent climatic research, including analysis of the historical record, indicates that major hurricanes [Category 3 or higher on the Saffir-Simpson scale (Simpson 1974)] may intensify in response to the warming sea surface temperatures (SST) associated with global warming (Elsner et al. 2008; Knutson and Tuleya 2008; Emanuel et al. 2008; Vecchi and Soden 2007; Webster et al. 2005). In this paper, the term hurricane intensity refers to hurricane central pressure. Through consideration of thermodynamic influences and evaluation of several convective parameterizations (Pan and

Wu 1995; Emanuel and Živković-Rothman 1999; Kurihara et al. 1998), Knutson and Tuleya (2004, 2008) estimated an average 8% increase in hurricane intensity for every 1°C of SST rise:

$$p_{\Delta SST} = p_o - 0.08\,(\Delta SST)\left(p_{far} - p_o\right) \tag{1}$$

where:

$p_{\Delta SST}$ is the future projected hurricane central pressure,
p_o is the present-day (or historical) hurricane central pressure,
ΔSST is the sea surface temperature change, and
p_{far} is the far-field barometric pressure.

The above approximation for hurricane intensification with SST change neglects other meteorological influences, such as wind shear, which can influence tropical system development into major hurricanes. Thus, Eq. 1 can be considered to represent hurricane intensity change with SST change for a future hurricane, should the tropical system fully develop. As will be shown later, the simplicity of Eq. 1 allows us to evaluate, in a general sense, the relative impact of hurricane intensification on surge generation.

2.2 Potential influence of global warming on sea level rise

Historical observations of global, or eustatic, mean sea level (MSL) indicate a net trend for SLR (IPCC 2007; National Oceanic and Atmospheric Administration [NOAA] 2008a; White et al. 2005; Miller and Douglas 2004). Historical eustatic SLR rates over the last century are reported to be 0.17 to 0.18 cm/year, whereas in recent years SLR shows acceleration to 0.30 cm/year (IPCC 2007). Global climate projections indicate that eustatic SLR may accelerate in response to global warming (IPCC 2007; Church and White 2006). The IPCC (2007) estimated an acceleration in SLR over historically observed rates. Based on the abovementioned IPCC future climate scenarios, the IPCC (2007) projected eustatic SLR between 0.18 and 0.60 m over the next century. However, some future eustatic SLR projections, such as those considering potentially catastrophic ice-sheet melting, estimate one 1 m or more of SLR over the next century (Pfeffer et al. 2008; Rahmstorf 2007; Otto-Bliesner et al. 2006); these conclusions regarding ice-sheet melting contributions have recently been substantiated through paeloclimatic analysis (Rohling et al. 2008). Here we adopt the IPCC climate projections (B1, A1B, A1FI) but acknowledge that if global warming induces significant ice-sheet melting, future SLR rates may be potentially higher than those considered in this paper.

2.3 Potential influence of global warming on coastal storm flooding

Increasing storm intensity and sea level both have implications on coastal flood elevations. In this paper, we focus on flood elevations at the coast where coastal surge dominates, and, as such, we will not consider rainfall-related flooding. Over the last few years, the increasing importance of SLR on coastal flooding has been studied. Kleinosky et al. (2007) reported on the relative role of SLR on future hurricane flooding along the mid-Atlantic coast of the USA, without consideration of potential hurricane intensification. These authors showed that flooding of critical facilities is

expected to increase by 1% to 19% for major hurricanes when SLR is between 0.3 and 0.9 m. Kirshen et al. (2008) considered the relative impact of SLR for non-tropical storms around Boston, Massachusetts, again without consideration of storm intensification, and concluded flood probability would increase substantially with a 0.6-m SLR; specifically, these authors conclude that the present-day 1%-occurrence flood level was projected to become the 26%-occurrence flood level by 2100. Similar findings were reported by Cayan et al. (2008) for the west coast of the U.S.

The coupled impact of both storm intensification and SLR has recently been investigated for non-tropical storms affecting the Atlantic coasts of Europe and Canada (Mitchell et al. 2006; Gonnert 2004; Danard et al. 2003; Demernard et al. 2002; Lowe et al. 2001). These studies show, for example, an increase in the present-day 1%-occurrence flood level in the North Sea to a 50%-occurrence flood level by the 2080s. Surges by major hurricanes are oftentimes significantly larger than surges generated by non-tropical weather events. However, research on the impact of hurricane intensification is limited. In the late 1990s, Ali (1996, 1999) reported climate projections of tropical cyclone flood levels in Bangladesh, where the projected SLR by the 2050s may potentially inundate about 15% of the country. Ali (1996, 1999) considered the impact of intensifying a stationary and uniform wind field combined with SLR and projected, on average, a 12% rise in Bay of Bengal flood levels per 1°C of SST rise.

The findings of (Ali 1996, 1999) also demonstrated that in shallow coastal areas, such as the Bay of Bengal, the influences of SLR and storm intensification must be evaluated together. A simplification of the momentum balance for surge generation shows that, for a constant wind (with speed V) acting over a water body of constant depth (h), the meteorologically generated surge (ζ) is:

$$\zeta \propto \frac{\tau_s}{h} \propto \frac{V^2}{h} \tag{2}$$

where τ_s is the wind momentum transfer into the water column, or wind stress. In Eq. 2, the second proportionality is based on the standard assumption that τ_s can be specified by the quadratic form $\rho_a c_d V^2$, where ρ_a is air density and c_d is wind drag coefficient. Equation 2 shows that any increase in mean water depth (e.g., SLR) is expected to decrease surge generation potential, while any increase in wind speed is expected to increase surge generation potential. The importance of SLR in Eq. 2 will depend on the relative amount of SLR with respect to initial depth. For example, in a shallow bay with a 4-m mean depth, a SLR of 0.5 m represents more than a 10% change in depth. However, along the open coast where the mean depth over which surge is generated may average 20 to 30 m, a SLR of 0.5 m will likely have no measurable impact on meteorological surge generation. It is important to note here that total flood elevation (z) will include both the meteorologically generated surge (ζ) plus the mean water level above some specified vertical datum, inclusive of any SLR.

Here, we investigate the coupled impact of potential SLR and hurricane intensification on coastal flooding for an area which includes open-coast locations and locations within a shallow-water bay, Corpus Christi, Texas. Unlike Ali (1996, 1999), we consider here realistic hurricane wind fields which vary spatially and are non-stationary. As will be discussed below, the wind-field spatial and temporal variability

are important as they alter the surge response from location to location and from storm to storm within coastal bays.

For these dynamic weather systems, it can be shown via numerical simulations (Planetary Boundary Layer [PBL] models: Vickery et al. 2000; Thompson and Cardone 1996) that the maximum hurricane wind speed scales with the square-root of the hurricane central pressure deficit ($p_{far} - p$, where p is the hurricane central pressure). Making this substitution and combining Eqs. 1 and 2, the relative influence of global warming on hurricane meteorological surge ($\zeta_{\Delta SST}$) is expected to scale as:

$$\zeta_{\Delta SST} \approx a\left[\frac{(1+0.08\Delta SST)\left(p_{far}-p_o\right)}{(h_o + SLR_{\Delta SST})}\right] + b \tag{3}$$

where:

h_o represents the present-day mean water depth,
$SLR_{\Delta SST}$ is the future projected SLR, and
a and b are constants.

The total future flood elevation, with respect to present-day (2000s) MSL (MSL_{2000s}), would then be:

$$z_{\Delta SST} = \zeta_{\Delta SST} + SLR_{\Delta SST} \tag{4}$$

where:

$z_{\Delta SST}$ is the future flood elevation with respect to MSL_{2000s}

In Eq. 4, the relative dependency between hurricane intensification and SLR is accounted for in the first term. In this paper, we will evaluate the potential impact of global warming on hurricane flooding in the context of Eqs. 3 and 4 using future climate projections based on the B1, A1B, and A1FI IPCC scenarios.

3 Study area

Of all coastal regions in the United States, the Gulf of Mexico is particularly vulnerable to high coastal surges. The relatively warm waters of the Gulf of Mexico promote hurricane activity, and the relatively shallow bathymetry often leads to high surge generation. Thus, selection of an urban community on the Gulf of Mexico is appropriate for evaluating the potential impact of global warming on coastal flooding. Corpus Christi, Texas, is situated along the northern Gulf of Mexico coastline (Fig. 1) and is regularly subjected to high hurricane surges. The City of Corpus Christi, on Corpus Christi Bay (mean depth of 3.5 m), can be separated into two regions: a mainland portion, which includes the downtown area, and a barrier island portion (Mustang Island). The barrier island is openly exposed to ocean surge, while the mainland portion of the city is exposed to surge waters which pass through Aransas Pass and to locally generated wind surge within the bay. Outside city limits are several smaller bayside communities, which include Ingleside and Portland. This populated stretch of the Texas coast has a diverse economic base. The Corpus Christi area is a popular tourist destination and houses a multitude of hotels, restaurants, and other hospitality-related businesses. This region also supports several petroleum

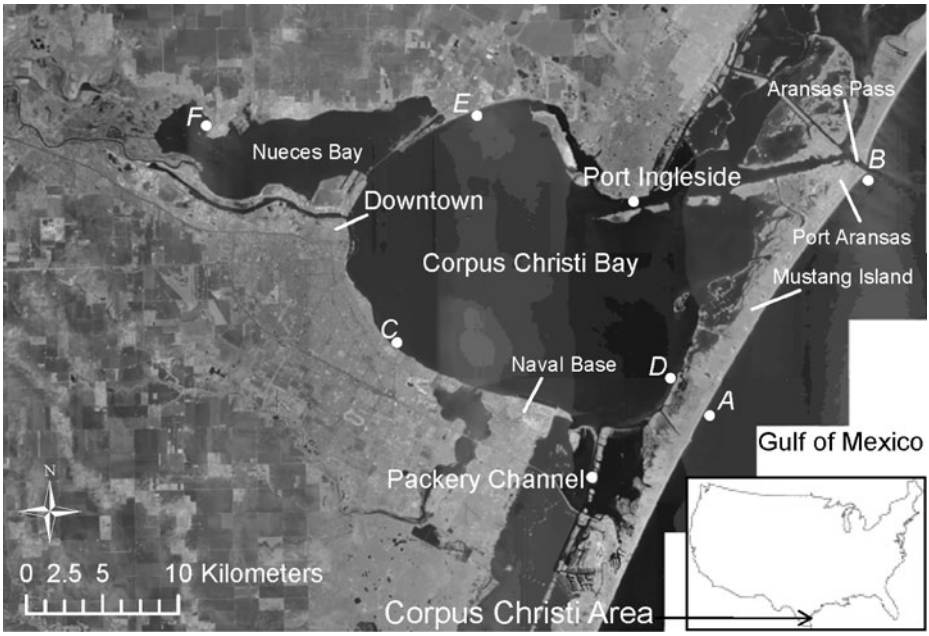

Fig. 1 Corpus Christi, Texas location map (aerial imagery from US Geological Survey 2008)

refineries and manufacturing plants, and is home to the Port of Corpus Christi and the Corpus Christi Naval Air Station.

In addition to being vulnerable to high hurricane surges, like much of the northern Gulf of Mexico coastline, the Corpus Christi region has historically experienced measurable land subsidence. Based on the difference between long-term mean water level observations near Corpus Christi (NOAA 2008a) and historical eustatic SLR rates (IPCC 2007), historical land subsidence rates are estimated to be 0.29 cm/year. This relatively high rate of land subsidence is expected to continue in this region.

3.1 Hurricane history and historical storm selection

To evaluate the impact of climate change on hurricane flooding, the historical hurricane record (NOAA 2008b) for the Texas coast was reviewed to identify three candidate major hurricanes for intensification using a PBL model, which uses as input hurricane central pressure, hurricane size, and hurricane position in time, among other parameters (Thompson and Cardone 1996). To reliably employ the PBL model to develop future realizations of intensified storms, each of the three selected historical hurricanes must be well described by an idealized vortex model. Namely, each storm should have a well-defined eye region with a classical hurricane wind field shape in which wind speed scales with radius from the center of the hurricane.

An additional restriction in storm selection was the ability to reliably determine historical hurricane parameters for the selected storms (e.g., central pressure, size). To meet this latter restriction, we considered only hurricanes occurring since the 1950s. Finally, because climatic research indicates potential intensification with global warming only for more intense, major hurricanes (Elsner et al. 2008), historical hurricane review is limited to major hurricanes.

Since 1950, ten major hurricanes have made landfall along the Texas coast. Those most affecting the Corpus Christi region are Hurricane Beulah (1967), Hurricane Allen (1980), and Hurricane Bret (1999). All three of these storms generated surges in excess of 1 m along the open coast (National Weather Service 2000; U.S. Army Corps of Engineers 1968; Lawrence and Kinberlain 2001), with Hurricane Allen producing surges as large as 3.7 m in some locations. Of these three hurricanes, two exhibit classical hurricane vortex characteristics (Beulah and Bret) and are ideally suited for meteorological estimation using a PBL model. The wind-field structure of Hurricane Allen, however, was highly complex, including a double eye configuration (e.g., NOAA 1983), making this storm unsuitable for studying the influence of hurricane intensification with a PBL model.

Hurricane Allen was the most significant hurricane surge event in Corpus Christi during the period considered here. To assess the relative impact of global warming over a range of surge events, a candidate high-surge event replacement hurricane was identified. Hurricane Carla (1961), while tracking to the north of Corpus Christi and generating relatively small surges in the study area, stands as one of the most severe hurricane surge events along the Texas coast. Other severe hurricane surge events along the Texas coast include the 1900 Galveston hurricane and Hurricane Ike in 2008; neither of these storms was considered here since limited meteorological information was available for the 1900 hurricane and Hurricane Ike occurred following completion of our study. To develop a "modified historical" surge event equivalent to Hurricane Carla for the Corpus Christi area, it was assumed that a hurricane of Hurricane Carla's intensity and size could have followed a more southerly track. While we acknowledge that if Hurricane Carla had actually taken a more southerly track in 1961, the exact hurricane parameters (size, intensity, etc.) would have varied somewhat from those on its actual track, we assume that no climatological or geographical reasons preclude a storm of the same intensity and size as Hurricane Carla from making landfall near Corpus Christi. Thus, the third hurricane selected for hurricane intensification analysis is Hurricane Carla shifted southward 130 km (Carla-shifted) such that maximum surge generation at the coast occurs at Corpus Christi (Irish et al. 2009; Irish and Resio 2010).

Table 1 summarizes selected hurricane parameters and observed hurricane surges for the three selected historical hurricanes. As indicated in the table, the three selected hurricanes span a range of hurricane surge potential and historical hurricane intensities.

It is worth noting that while Hurricanes Beulah and Bret were characterized by similar hurricane central pressures, around 950 mb, the aerial extent (storm radius) of Hurricane Beulah was substantially larger than that of Hurricane Bret. In consequence, Hurricane Beulah generated about twice as much surge as Hurricane Bret. Since climatic research to date has not indicated a trend in hurricane size with global warming, size will not be considered as a climatic variable here, although it is recognized that storm size influences surge generation (Irish et al. 2008a).

Table 1 Historical hurricane parameters at landfall

Storm name	Central pressure (mb)[a]	Radius to maximum wind (km)[b]	Saffir–Simpson (Simpson 1974) category[c]	Landfall distance from Corpus Christi (km)	Observed ocean side surge (m)
Carla (1961)	931	56	4	85 (northeast)	3.3–3.7[d]
Beulah (1967)	950	46	3	95 (south)	2.4–2.9[e]
Bret (1999)	951	19	3	200 (south)	0.9–1.5[f]

[a]National Weather Service (2000)
[b]US Army Corps of Engineers (2006)
[c]Blake et al. (2006)
[d]Ho and Miller (1982), surge corresponds to historical observations for Hurricane Carla on historical track
[e]US Army Corps of Engineers (1968)
[f]Lawrence and Kinberlain (2001)

4 Future global warming scenarios

To evaluate potential future hurricane flooding over the next 80 years, 6-month-average projections of changes in ΔSST were developed for two periods, the 2030s and the 2080s, using the climate model MAGICC/SCENGEN (Wigley 2004), with a base year of 1990, and assuming three IPCC future climate scenarios: B1, A1B, and A1FI. For each of the three future climate scenarios, three carbon dioxide doubling sensitivity tests were evaluated (2°C, 3°C, and 4.5°C), so that a total of 54 estimates were made with the MAGICC/SCENGEN model. Figure 2 (top pane) summarizes the climate model projections by showing the range of projected SST by decade. As shown in this figure, by the 2030s, SST is projected to rise between 0.01°C/year (low rate of warming) and 0.06°C/year (high rate of warming). By the 2080s, these climate projections indicate on the order of ΔSST = 1 to 5°C, with respect to present-day (2000s) conditions.

In this analysis, future hurricanes were assumed to occur as they did historically, except for the track shift for Hurricane Carla, but with higher SSTs and sea levels. Future hurricane intensity scenarios were developed using Eq. 1, by applying the climate model projections for SST rise to the historically observed hurricane central pressure time histories for the three selected historical hurricanes (Fig. 2, center pane). The future intensification projections for storms like Hurricane Carla are most dramatic, with an intensification of 0.14 to 0.45 mb/year. The most extreme future projection for Hurricane Carla (A1FI [high rate of warming] for the 2080s) gives a central pressure at landfall of 899 mb. Future projections of storms like Hurricanes Bret and Beulah show rates of intensification between 0.07 and 0.32 mb/year.

The MAGICC/SCENGEN climate model was also used to project future eustatic SLR based on the three IPCC scenarios; again, three carbon dioxide doubling sensitivity tests per climate scenario were evaluated. These projections (Fig. 2, bottom pane) indicate eustatic SLR rates of 0.08 cm/year (low rate of warming) to 0.29 cm/year (high rate of warming). With a high rate of warming (A1FI), eustatic SLR by the 2080s is expected to be as much as 58.4 cm, with respect to present-day (2000s) sea level. It is worth noting again that the SLR scenarios considered here could be much higher with major ice sheet melting.

As mentioned previously, the Corpus Christi region experiences a relatively large rate of land subsidence (about 0.29 cm/year). Assuming that the historical subsidence

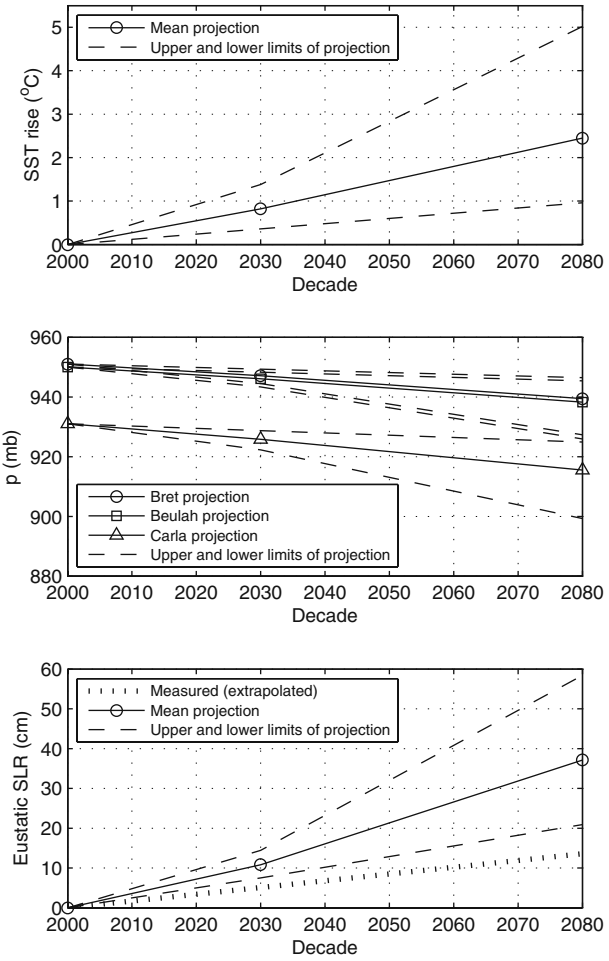

Fig. 2 Projected sea surface temperature (SST) rise (*top pane*), projected hurricane intensification at landfall (*center pane*), and projected eustatic sea level rise (SLR; *center pane*)

rate continues into the future, between the 2000s and the 2030s and 2080s an additional SLR of 8.4 and 22.4 cm, respectively, above the eustatic SLR is estimated for this region. Thus, based on the mean eustatic SLR projections, the relative SLR between the 2000s and the 2030s and 2080s is estimated to be about 19 and 60 cm, respectively. With the high rate of warming (A1FI), the total relative SLR by the 2080s is projected to be as high as 80.8 cm, with respect to MSL_{2000s}.

5 Numerical simulation approach

By considering the abovementioned projected relative SLR and projected hurricane intensification scenarios for the Corpus Christi area, flood levels were estimated using a surge response function (SRF) approach (Irish et al. 2009). In this analysis, three historical hurricanes are considered in which future projections of each hurricane hold constant the time history of storm position, size, forward speed, and

approach angle. In other words, the only variables driving surge level change are the hurricane's intensity (p) and the relative SLR. Within this framework, SRFs were developed by numerical simulation for each of the three historical hurricane scenarios (Table 1). These simulations provide a basis to define the flood elevation as a function of global warming, namely projections of p and SLR, where the form of the SRFs is given in Eq. 3. An advantage of the SRF approach is that the SRF, along with Eq. 4, may be used to estimate the flood elevation response associated with any future climate projection that falls within the p-SLR parameter space. Thus, while we have adopted the B1, A1B, and A1FI of the IPCC for discussion here, the SRFs may be used to evaluate any alternate climate scenario for any future period of interest.

Anticipating that the scaling relationship in Eq. 3 holds, numerical hurricane surge simulations were carried out for a discrete set of hurricane scenarios which spanned the projected p-SLR parameter space and provided sufficient representation of intermediate intensification-SLR conditions (Table 2). In all, 23 hydrodynamic simulations were carried out, where seven to eight p-SLR conditions were considered for each of the three selected storms (Bret, Beulah, and Carla-shifted).

Table 2 Hurricane scenarios for numerical simulation

Central pressure at landfall (mb)	Relative SLR (cm)	Simulated flood elevation, z (m, MSL_{2000s})					
		A	B	C	D	E	F
Hurricane Bret							
951	0.0	0.74	0.66	0.97	0.47	0.84	1.80
951	75.0	1.48	1.40	1.62	1.24	1.48	2.26
935	0.0	0.93	0.82	1.18	0.59	1.02	2.15
935	31.0	1.24	1.12	1.45	0.89	1.28	2.32
925	0.0	1.04	0.90	1.29	0.65	1.12	2.31
925	37.5	1.41	1.27	1.61	1.03	1.43	2.52
925	75.0	1.78	1.64	1.92	1.43	1.74	2.74
Hurricane Beulah							
950	0	1.08	0.98	1.68	1.07	1.52	2.93
950	37.5	1.45	1.35	1.97	1.47	1.85	3.13
950	75.0	1.82	1.72	2.26	1.88	2.21	3.33
933	0.0	1.32	1.19	1.96	1.30	1.80	3.38
933	31.0	1.62	1.49	2.19	1.62	2.07	3.53
924	0.0	1.47	1.32	2.13	1.44	1.97	3.64
924	37.5	1.83	1.68	2.40	1.82	2.30	3.82
924	75.0	2.20	2.05	2.68	2.23	2.66	4.02
Hurricane Carla (shifted)							
931	0.0	3.23	3.10	3.19	1.66	3.03	4.89
931	75.0	3.93	3.80	3.69	2.25	3.63	5.33
923	0.0	3.50	3.36	3.35	1.76	3.21	5.14
911	0.0	3.91	3.73	3.56	1.89	3.44	5.42
911	31.0	4.19	4.01	3.76	2.14	3.67	5.61
900	0.0	4.26	4.06	3.74	1.99	3.63	5.64
900	37.5	4.61	4.40	3.98	2.28	3.94	5.89
900	75.0	4.95	4.75	4.21	2.55	4.24	6.11

See Fig. 1 for locations A through F

The shallow-water hydrodynamic model ADCIRC (ADvanced CIRCulation; Luettich and Westerink 2008) was used to simulate hurricane flood elevations for each hurricane condition in Table 2. ADCIRC is a finite-element hydrodynamic model designed for simulating currents and water levels resulting from tidal, wind, and ocean wave forcing. The two-dimensional depth-integrated version of ADCIRC solves the shallow-water equations for conservation of mass (Eq. 5) and momentum (Eq. 6):

$$\frac{\partial H}{\partial t} + \nabla_H \left(\overrightarrow{U} H \right) = 0 \tag{5}$$

$$\frac{\partial \overrightarrow{U}}{\partial t} + \left(\overrightarrow{U} \cdot \nabla_H \right) \overrightarrow{U} = -g \nabla_H \left(\zeta_2 + \frac{p\,(x,\,y)}{g\rho_w} - \alpha\eta \right) + f \overrightarrow{k} \times \overrightarrow{U} + \frac{\overrightarrow{\tau_s}}{H\rho_w} - \frac{\overrightarrow{\tau_b}}{H\rho_w} \tag{6}$$

where:

ζ_2	is the instantaneous free surface elevation,
H	is the total depth ($h(x, y) + \zeta_2$, where $h(x, y)$ is the spatially variable still water depth),
U	is the depth-integrated horizontal velocity,
$p(x, y)$	is the spatially variable atmospheric pressure,
ρ_w	is the density of water,
f	is the Coriolis parameter,
k	is the horizontal unit vector, and
τ_b	is the bottom shear stress.

The ADCIRC model grid spans the Gulf of Mexico and the northeastern Atlantic Ocean from 60° W to 98° W in longitude and between 8° N and 46° N in latitude in order to adequately simulate storm surge by large weather events like hurricanes. The grid resolution within the study area (nearshore and Corpus Christi Bay) is sufficiently refined (as fine as 70 m within channels) to simulate the surge response to local geographic and bathymetric features, where grid bathymetry was based on multiple measurement sources (US Army Corps of Engineers 2006; M. Brown, personal communications). Model performance for surge prediction has been shown to be within 15 cm with respect to historical observations (Irish et al. 2008b).

For computational efficiency, three simplifying assumptions were made in projecting relative changes in hurricane flooding with global warming. First, the additional contributions to hurricane flooding by wave setup (by momentum transfer to water column when waves break near the coast) were not considered. While wave setup can contribute measurably to flood levels (Dean and Bender 2006, Irish and Cañizares 2009), the relative change in wave setup with global warming is expected to scale with changes in meteorological surge. Second, the relative impact of astronomical tide variation within the study area was assumed to have negligible impact on meteorological surge generation. The measured tidal range in the Corpus Christi region is 40 cm along the open coast and 10 cm within Corpus Christi Bay (NOAA 2008a). The mean bay depth is 3.5 m, and the bulk of surge generation along the open coast occurs in depths shallower than about 30 m (Irish and Resio in review). Thus, the depth change with tide is about 2%. Here, we assume the variation with astronomical

tide may be added to the simulated flood level, based on hurricane meteorology and relative SLR. Finally, we assume the barrier island system fronting Corpus Christi Bay is static, such that storm morphodynamics and any resulting influence of barrier-island overwash and breaching on flood levels is not considered. We acknowledge that barrier island overflow can elevate flood levels during hurricanes (Cañizares and Irish 2008); however, an evaluation of storm morphodynamics is beyond the scope of this paper.

To evaluate meteorological surge, for each of the 23 hurricane scenarios ADCIRC was forced throughout its computational domain using time-stepping surface wind stress (τ_s) and barometric pressure fields [$p(x, y)$] developed using a PBL model (Thompson and Cardone 1996). Each meteorological input file was generated on a grid with 2-km spacing in both latitude and longitude. The southwest and northeast grid locations were 98° W, 18° N and 80° W, 31° N, and the meteorological input was generated at 15-min intervals. To evaluate the relative impact of changing MSL, the mean water level within the model was specified based on the relative SLR scenario being evaluated.

6 Results

The hydrodynamic simulations show a relative rise in hurricane flood elevations at all locations within the study region in response to both projected hurricane intensification and projected relative SLR. Table 2 shows simulated peak flood elevations at six locations in the Corpus Christi region. As discussed below, within the study area, the relative importance of hurricane intensification and the relative importance of SLR with location and geography were quantified separately. In the following discussion, two definitions of storm water level will be used. The term "surge" will refer to the meteorologically generated surge only (ζ; i.e., does not include SLR) while the term "flood elevation" will refer to the total water elevation (z) inclusive of surge (ζ) and SLR.

6.1 Impact of hurricane intensification on hurricane surge

The subset of simulations in Table 2 when SLR = 0 cm provides a means for quantifying the relative change in hurricane surge with change in hurricane intensity only. Figure 3 presents representative hurricane surge time series for three Hurricane Beulah intensity scenarios. As expected, this figure shows that hurricane surge increases with hurricane intensification, and that this trend is evident over the duration of hurricane passage. Over the 1-day period around the peak surge, at all locations, hurricane surge increased 10% to 15% per 10 mb of central pressure drop. At both ocean locations (A and B), the timing of peak surge nearly coincided with hurricane landfall, and both ocean locations show similar surge magnitude and time series shape. For locations within Corpus Christi Bay, the timing of peak surge, and the magnitude of peak surge, vary as a function of localized wind setup effects. Surge magnitude within the bay is generally higher than that on the ocean side for all bay locations and for all hurricane scenarios considered. As a hurricane makes landfall in this region, easterly winds tend to push water to the west, thereby increasing surge levels at western locations (e.g., F) and decreasing surge levels at eastern locations

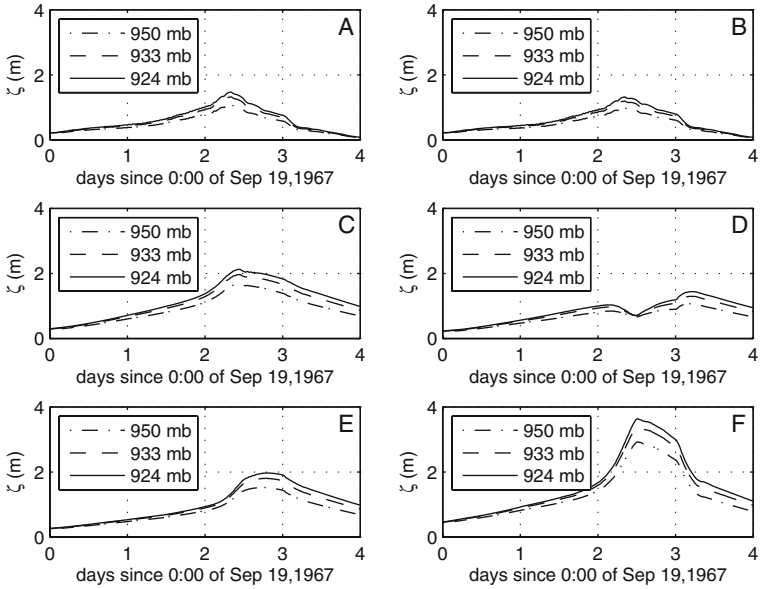

Fig. 3 Hurricane surge (meteorological only) time series for hurricanes like Hurricane Beulah when MSL = MSL_{2000s}. Simulation output locations are shown in Fig. 1

(e.g., D). At locations C, E, and F, peak surge lags the peak ocean side surge by 2 to 9 h, and surge subsides as the storm moves landward away from the bay. In contrast, peak surge at eastern locations (e.g., D) is not realized until after hurricane passage. Here, highest surge levels occur once hurricane-force winds are removed from the bay, thus allowing surge waters to slosh back to the east. At location D, peak surge lags ocean side surge by almost one day and underscores the importance of considering both spatial and temporal wind-field variability when determining hurricane surge. As will be discussed below, this phenomenon is also important when determining the relative impact of SLR on hurricane surge generation.

The trends discussed here for Hurricane Beulah are, in general, similar to those trends observed for Hurricanes Bret and Carla (shifted) with the most notable differences being the relative magnitude of the hurricane surge response. As anticipated, the increase in hurricane surge is relatively smaller (in absolute terms) for Hurricane Bret scenarios and relatively larger for Hurricane Carla (shifted) scenarios (Table 2). Another difference is in the eastern bay response during the Hurricane Carla (shifted) scenarios where two peaks in surge are observed: one coincides with the hurricane landfall while the other coincides with the sloshing back of surge waters following subsidence of hurricane-force winds. While these two peaks are of similar magnitude, the peak coinciding with hurricane landfall is slightly larger.

Figure 4 shows representative peak surge level maps for three Hurricane Beulah intensity scenarios when MSL = MSL_{2000s} (i.e., no SLR). As seen in this figure, surge increases as the hurricane is intensified everywhere within Corpus Christi Bay and along the open coast. This figure illustrates two important contributions to surge levels within Corpus Christi Bay as hurricanes intensify. First, the volume of water entering the bay from the ocean through Aransas Pass increases with increasing

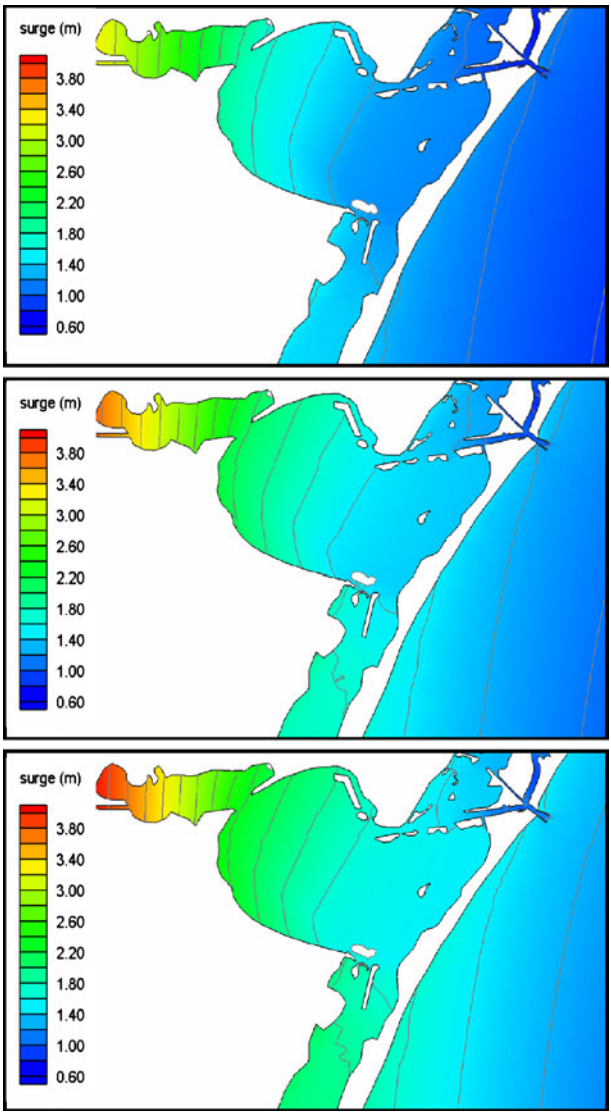

Fig. 4 Peak hurricane surge (ζ) maps for hurricanes like Hurricane Beulah when MSL = MSL_{2000s} (i.e., SLR = 0 cm) and hurricane intensity is $p = 950$ mb (*top pane*), 933 mb (*center pane*), and 924 mb (*bottom pane*). *Contour lines* are drawn every 0.2 m

hurricane intensity. This is evidenced by the net rise in spatially averaged surge level within the bay as hurricane intensity is increased. For the Hurricane Beulah scenarios, the spatially averaged peak surge within Corpus Christi Bay rises with the ocean side peak surge (within 2 cm of peak surge at location A), increasing 16 cm per 10-mb drop in hurricane central pressure.

Second, the impact of local wind setup becomes more pronounced with increasing hurricane intensity. Specifically, the slope in peak surge along the length of the bay, from west to east, becomes steeper as hurricane central pressure drops. This local wind setup results in relatively higher surges in the western portion of the bay and relatively lower surges in the eastern portion of the bay. For the Hurricane Beulah

scenarios, at western location F, for example, surge rises an additional 11 cm per 10-mb pressure drop over the spatially averaged rise rate of 16 cm/10 mb (total rise of 27 cm/10 mb). At eastern location D, surge drops 2 cm/10 mb with respect to the spatially averaged rise rate (total rise of 14 cm/10 mb). At centrally positioned bay locations (e.g., locations C and D), the total rise in surge is nearly equivalent to the spatially averaged rise rate of 16 cm/10 mb. This finding indicates the importance of considering local geometry and wind-field evolution when evaluating surge response to future hurricane intensification. It is anticipated that both the location of the point of interest and the general coastal bay characteristics will determine the relative rise in surge level with hurricane central pressure drop. For Hurricanes Bret and Carla (shifted), the trends in surge distribution throughout Corpus Christi Bay and in surge response to hurricane intensification are similar to those discussed here for Hurricane Beulah.

6.2 Impact of sea level rise on hurricane surge

Table 2 shows projected peak flood elevations for a subset of simulations that consider the relative impact of SLR on surge generation while holding hurricane central pressure constant. These simulations elucidate the relative importance of SLR on hurricane surge generation. Figure 5 shows representative differences between simulated flood elevation time series when SLR is dynamically included in the hydrodynamic simulation [z(SLR)] and the simulated flood elevation time series

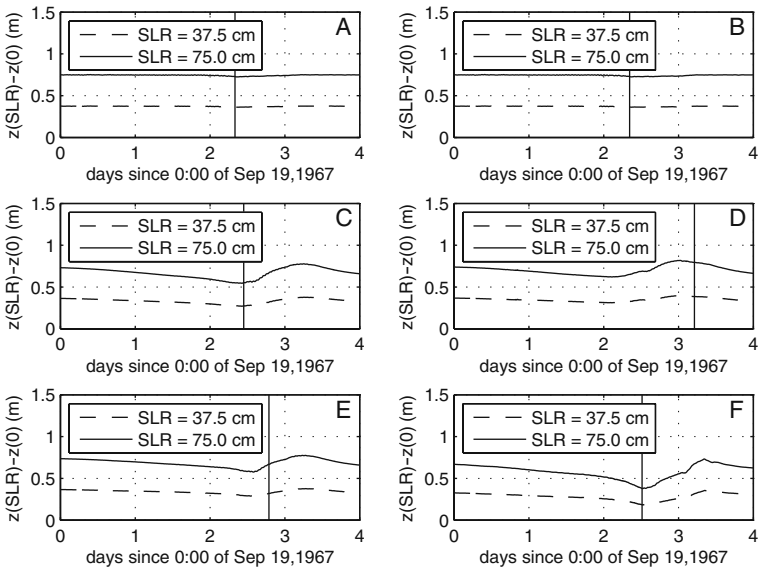

Fig. 5 Net change in hurricane flood elevation (z) time series versus SLR for hurricanes like Hurricane Beulah when $p = 924$ mb; time of peak surge is indicated by a vertical line. Simulation output locations are shown in Fig. 1

when SLR = 0 [$z(0)$], for the extreme Hurricane Beulah scenario when hurricane intensity is held constant at c_p = 924 mb. In this figure, if SLR does not change meteorological surge generation, the flood elevation difference should equal the amount of SLR: $z(\text{SLR}) - z(0) = \text{SLR}$. If instead the percent change in mean depth for surge generation is substantial, the quantity $z(\text{SLR}) - z(0)$ will differ from the amount of SLR (e.g., Eq. 3). Figure 5 shows that along the open coast, where depths are generally greater, SLR has negligible impact on meteorological surge development (less than 2% at peak surge). This finding holds for all hurricane intensity–SLR scenarios considered here (Table 2).

In contrast, within the shallow coastal bay, SLR changes the surge response (Figs. 5 and 6). At western bay locations (C, E, and F), there is a relative reduction in peak surge. The amount of this reduction increases nonlinearly with SLR. At locations in the eastern portion of the bay (e.g., location D), a slight reduction in the surge time series is predicted during the time of storm passage over the bay (at 2 to 3 days). However, the time of peak surge at this location occurs after hurricane-force winds subside and surge waters slosh back to the east. At this time (3.2 days), a relative increase in surge is predicted. So at location D, the estimated flood level is greater than the sum of the surge prediction (without SLR) plus SLR. The magnitude of this surge increase is small (less than 2 cm). The observed trends in surge time series for the Hurricane Beulah scenarios are similar to those for the Hurricane Bret and Hurricane Carla (shifted) scenarios. One notable exception relates to eastern bay locations for the Hurricane Carla (shifted) scenarios. As discussed in the previous section, the first of two surge peaks at this location dominates slightly, and this peak coincides with a relative lowering of surge with SLR.

6.3 Flood elevation rise with global warming

The hydrodynamic simulation data were analyzed using Eq. 3 to develop SRFs, which account for the dynamic coupling between relative SLR and hurricane intensification. Figure 7 shows the simulated meteorological surge ($\zeta_{\Delta SST}$) as a function of the ΔSST-SLR term in Eq. 3. In evaluating this ΔSST-SLR term, the present-day mean water depth, h_o, was taken as 3.5 m for bay locations and 30 m (characteristic) for ocean-side locations. As anticipated, a nearly linear trend with the ΔSST-SLR

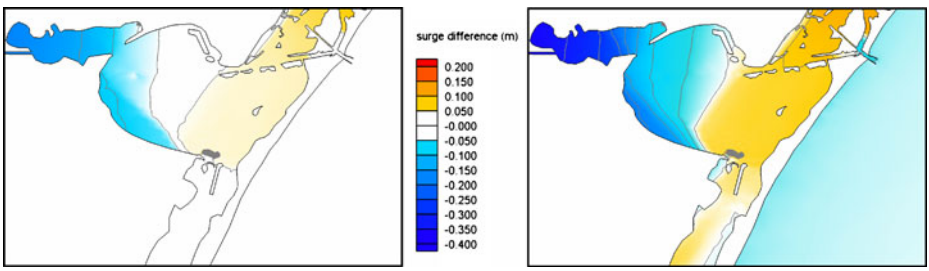

Fig. 6 Maps of net change in peak hurricane surge (ζ) when relative SLR is 37.5 cm (*left pane*) and 75.0 cm (*right pane*), with respect to surge when MSL = MSL_{2000s} (i.e., no SLR), for the most intense scenario of Hurricane Beulah (p = 924 mb). Contour lines are drawn every 0.05 m (5 cm) where negative values represent a reduction in surge with SLR and positive values represent an increase in surge with SLR

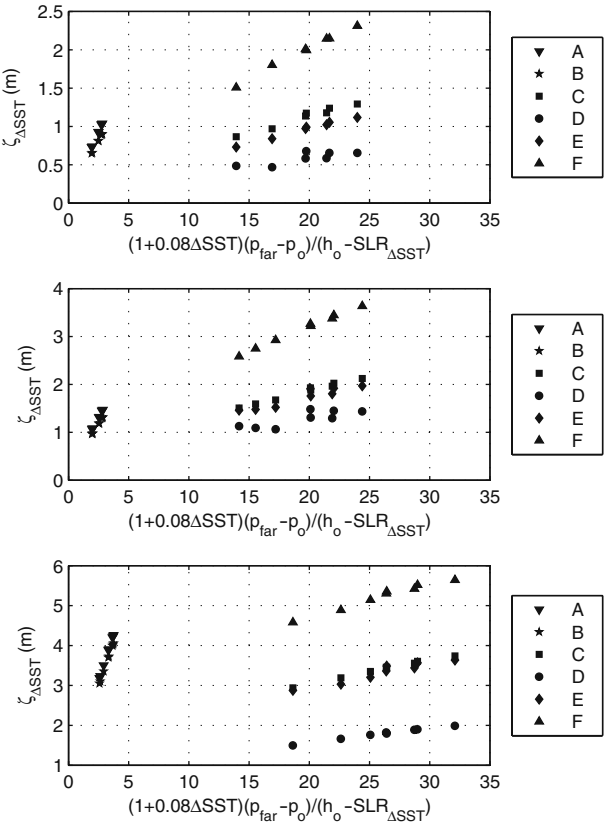

Fig. 7 Surge response functions (SRF) at selected location (see Fig. 1) for storms like Hurricanes Bret (*top pane*), Beulah (*center pane*), and Carla (shifted; *bottom pane*)

term is indicated at all locations, both along the open coast and within Corpus Christi Bay, confirming the SRF form is well-described by Eq. 3. By taking best-fit lines through the simulated data at each location, the location- and storm-dependent constants (a, b) in Eq. 3 were determined (Table 3). The best-fit lines have an R^2 of 0.90 or better for all locations and for all three hurricanes, with the exception of location D for Hurricane Beulah where R^2 is 0.70. These SRFs, along with Eq. 4, were then used to evaluate future projections of flood elevation based on the IPCC

Table 3 Surge response function (SRF) constants for selected location (see Fig. 1)

Location	Hurricane Bret		Hurricane Beulah		Hurricane Carla (shifted)	
	a (m^2mb^{-1})	b (m)	a (m^2mb^{-1})	b (m)	a (m^2mb^{-1})	b (m)
A	0.36	0.03	0.47	0.15	0.94	0.76
B	0.30	0.07	0.41	0.18	0.87	0.81
C	0.04	0.25	0.06	0.63	0.06	1.83
D	0.02	0.19	0.04	0.52	0.04	0.83
E	0.04	0.19	0.06	0.64	0.06	1.72
F	0.08	0.43	0.10	1.15	0.08	3.06

Table 4 Projected flood elevations corresponding with IPCC-based future climate projections for Hurricane Bret

Climate Scenario	ΔSST (°C)	Flood elevation (m, MSL_{2000s}) [Flood elevation rise (m)]					
		A	B	C	D	E	F
2030s							
B1	0.51–1.38	0.9–1.1	0.8–1.0	1.1–1.3	0.7–0.8	1.0–1.1	2.0–2.1
		[0.2–0.3]	[0.2–0.3]	[0.2–0.3]	[0.2–0.3]	[0.2–0.3]	[0.2–0.3]
A1B	0.40–1.30	0.9–1.1	0.8–1.0	1.1–1.3	0.7–0.8	1.0–1.1	1.9–2.1
		[0.2–0.3]	[0.2–0.3]	[0.2–0.3]	[0.2–0.3]	[0.2–0.3]	[0.1–0.3]
A1FI	0.36–1.23	0.9–1.0	0.8–1.0	1.1–1.3	0.6–0.7	1.00–1.1	1.9–2.1
		[0.2–0.3]	[0.2–0.3]	[0.2–0.3]	[0.2–0.3]	[0.2–0.3]	[0.1–0.3]
2080s							
B1	0.96–2.81	1.2–1.6	1.1–1.4	1.4–1.7	1.0–1.2	1.3–1.6	2.2–2.5
		[0.5–0.8]	[0.5–0.8]	[0.4–0.8]	[0.5–0.8]	[0.4–0.7]	[0.4–0.7]
A1B	1.28–3.80	1.3–1.7	1.19–1.56	1.5–1.8	1.0–1.4	1.3–1.7	2.2–2.6
		[0.6–0.9]	[0.5–0.9]	[0.5–0.9]	[0.5–0.9]	[0.5–0.8]	[0.4–0.8]
A1FI	1.64–5.02	1.4–1.8	1.3–1.7	1.5–2.0	1.1–1.5	1.38–1.77	2.3–2.8
		[0.6–1.1]	[0.6–1.0]	[0.6–1.0]	[0.6–1.0]	[0.5–0.9]	[0.5–0.9]

future climate scenarios considered here (Tables 4, 5 and 6). These tables show that, at all locations in the Corpus Christi region, the projected impact of global warming is an increase in hurricane flood level, regardless of climate projection scenario. At a minimum, flood elevations for major hurricanes are projected (mean of projections) to rise about 0.3 and 0.8 m by the 2030s and 2080s, respectively.

Based on the IPCC-based climate projections for the 2030s and 2080s, the impact of SLR on hurricane flooding along this stretch of open coast (e.g., locations A and B) is slightly more important than the impact of surge rise by hurricane intensification for moderate to large surge events like the Hurricane Bret and Beulah scenarios. Here, SLR makes up between 60% and 70% of the flood elevation rise and hurricane

Table 5 Projected flood elevations corresponding with IPCC-based future climate projections for Hurricane Beulah

Climate Scenario	ΔSST (°C)	Flood elevation (m, MSL_{2000s}) [Flood elevation rise (m)]					
		A	B	C	D	E	F
2030s							
B1	0.51–1.38	1.3–1.4	1.2–1.3	1.8–2.0	1.3–1.4	1.7–1.8	3.1–3.0
		[0.2–0.3]	[0.2–0.3]	[0.2–0.3]	[0.2–0.3]	[0.2–0.3]	[0.2–0.3]
A1B	0.40–1.30	1.3–1.4	1.2–1.3	1.8–2.0	1.3–1.4	1.7–1.8	3.1–3.0
		[0.2–0.3]	[0.2–0.3]	[0.2–0.3]	[0.2–0.3]	[0.2–0.3]	[0.2–0.3]
A1FI	0.36–1.23	1.3–1.4	1.2–1.3	1.8–2.0	1.3–1.4	1.7–1.8	3.1–3.2
		[0.2–0.3]	[0.2–0.3]	[0.2–0.3]	[0.2–0.3]	[0.2–0.3]	[0.2–0.3]
2080s							
B1	0.96–2.81	1.6–1.9	1.5–1.8	2.1–2.4	1.6–2.0	2.0–2.3	3.3–3.6
		[0.5–0.8]	[0.5–0.8]	[0.4–0.7]	[0.5–0.9]	[0.5–0.8]	[0.4–0.7]
A1B	1.28–3.80	1.6–2.1	1.5–1.9	2.2–2.5	1.7–2.1	2.1–2.5	3.3–3.8
		[0.6–1.0]	[0.5–0.9]	[0.5–0.9]	[0.6–1.0]	[0.5–1.0]	[0.4–0.9]
A1FI	1.64–5.02	1.7–2.2	1.6–2.1	2.2–2.7	1.7–2.3	2.1–2. 7	3.4–4.0
		[0.6–1.1]	[0.6–1.1]	[0.5–1.0]	[0.7–1.2]	[0.6–1.2]	[0.5–1.1]

Table 6 Projected flood elevations corresponding with IPCC-based future climate projections for Hurricane Carla (shifted)

Climate Scenario	ΔSST (°C)	Flood elevation (m, MSL_{2000s}) [Flood elevation rise (m)]					
		A	B	C	D	E	F
2030s							
B1	0.51–1.38	3.5–3.7	3.4–3.6	3.4–3.5	1.8–2.0	3.3–3.4	5.1–5.3
		[0.3–0.5]	[0.3–0.5]	[0.2–0.3]	[0.2–0.3]	[0.2–0.4]	[0.2–0.4]
A1B	0.40–1.30	3.5–3.7	3.3–3.6	3.4–3.5	1.8–1.9	3.2–3.4	5.1–5.3
		[0.2–0.5]	[0.2–0.7]	[0.2–0.3]	[0.2–0.3]	[0.2–0.4]	[0.2–0.4]
A1FI	0.36–1.23	3.5–3.7	3.3–3.6	3.3–3.5	1.8–1.9	3.2–3.4	5.1–5.3
		[0.2–0.5]	[0.2–0.5]	[0.2–0.3]	[0.2–0.3]	[0.2–0.4]	[0.2–0.4]
2080s							
B1	0.96–2.81	3.8–4.4	3.7–4.3	3.6–3.9	2.1–2.4	3.5–3.9	5.3–5.8
		[0.6–1.2]	[0.6–1.2]	[0.4–0.8]	[0.4–0.7]	[0.5–0.9]	[0.5–0.9]
A1B	1.28–3.80	4.0–4.7	3.8–4.5	3.7–4.1	2.1–2.5	3.6–4.1	5.1–6.0
		[0.7–1.5]	[0.7–1.4]	[0.5–0.9]	[0.5–0.8]	[0.6–1.1]	[0.5–1.1]
A1FI	1.64–5.02	4.1–5.0	3.9–4.8	3.7–4.3	2.2–2.0	3.7–4.3	5.5–6.2
		[0.8–1.8]	[0.8–1.7]	[0.5–1.1]	[0.5–0.9]	[0.6–1.3]	[0.6–1.3]

intensification makes up the remaining 30% to 40%. This is evidenced by a relative rise in flood level of between 0.2 and 0.3 m by the 2030s and between 0.5 and 1.1 m by the 2080s, depending on climate projection, when projected relative SLR for the 2030s is around 0.2 m, and for the 2080s is between 0.4 and 0.8 m. The projected rise in meteorological surge by the 2030s contributes less than 0.1 m to flood elevations for these moderate to severe surge events. By the 2080s, projected rise in meteorological surge contributes between 0.1 and 0.3 m to total flood elevation. It is worth noting, however, that the relative contribution to flooding by hurricane intensification will likely be more important in locations characterized by wider continental shelves which promote more surge generation, such as along the northeastern Texas coast.

Within the bays, the flood response with global warming is more complex owing to the dynamic interaction between deepening of the shallow bay by SLR and hurricane intensification, as described above. However, the net change in flood elevation magnitude at most bay locations for the moderate to severe flood events considered here (Bret and Beulah) is on the order of the net change at open coast locations, where eastern bay locations (e.g., Location F) are slightly less sensitive to global warming.

For very intense, large hurricanes producing catastrophic-type surge conditions, like the Hurricane Carla (shifted) scenarios, the impact of surge rise by hurricane intensification and the impact of SLR more equally contribute to change in projected flood elevations at open coast locations in the Corpus Christi region. Here, open coast flood elevations are projected to rise between 0.2 and 0.5 m by the 2030s, when the projected rise in meteorological surge contributes between 0.1 and 0.3 m to flood elevation rise. By the 2080s, open coast flood elevations are projected to rise between 0.6 and 1.8 m, with rise in meteorological surge contributing 0.2 to 1.0 m to flood elevation rise. Based on 2030s and 2080s projections, changes in spatial mean bay flood elevation are about 0.1 and 0.3 m lower, respectively, than ocean side flood elevation, most likely due to constriction of the inlet limiting the flow of ocean waters into the bay.

7 Discussion and conclusions

The hydrodynamic simulation results show that, if future global warming projections are realized, the rise in hurricane flood elevations can be significant. In low-lying coastal regions like the barrier island portion of Corpus Christi, TX flood elevation changes on the order of those projected for the 2030s (0.3 m on average) can result in wider-spread flood inundation and more economic damages. In highly populated coastal regions, like the downtown area of Corpus Christi, the potential impact of global warming on coastal flooding can be severe, resulting in families and businesses being displaced following major hurricane events.

The numerical simulations also show that the relative rise in flood elevation with global warming can reasonably be described by a simple function of hurricane intensification (central pressure) and SLR (i.e., Eq. 3). This finding provides a means to simplify evaluation of potential global-warming-induced flooding in other coastal areas.

It is worth mentioning that the flood elevation rise values presented here, particularly within Corpus Christi Bay, may understate the potential increase in hurricane flooding resulting from global warming. First, the hydrodynamic simulations did not include storm water contributions to bay flood levels arising from flow over the barrier islands due to storm-induced overwash and breaching. Second, wave setup contributions were not considered in this analysis. It is expected that for large, intense hurricanes wave conditions will likely reach an equilibrium state such that further intensification will minimally alter the wave climate at the coast (Irish et al. 2008b). However for smaller, less intense hurricane (e.g., Hurricane Bret), some increase in wave height, and thus wave setup, is expected with hurricane intensification. Third, some future warming projections indicate higher rates of eustatic SLR (Rahmstorf 2007; Pfeffer et al. 2008), while some hurricane potential theories (Holland 1997) indicate higher rates of hurricane intensification with temperature rise, both of which would lead to higher flood elevations.

In conclusion, we have shown here that the potential impact of global warming on hurricane flooding can be substantial, with flood elevations expected to rise approximately 0.3 and 0.8 m by the 2030s and 2080s, respectively. We have also demonstrated that both SLR and hurricane intensification should be considered when evaluating potential future hurricane flood conditions. For the Corpus Christi region, specifically, SLR and hurricane intensification nearly equally contribute to flood elevation rise along the open coast. If these future projections are realized, hurricane events will cause more widespread inundation and damages in the study region and carry with them wide-reaching regional and national economic consequences.

Acknowledgements This research was supported by the National Commission on Energy Policy (Grant No. C07-00604). The authors wish to thank Oceanweather, Inc. for allowing use of their Planetary Boundary Layer model and the US Army Engineer Research and Development Center for providing the ADCIRC grid for the Corpus Christi region. The authors also wish to thank Mr. Joel Smith and Stratus Consulting, Inc. for providing guidance on hurricane intensification determination, sea surface temperature and sea level rise projections, and review of this manuscript.

Nomenclature

surge	Meteorologically generated surge
flood elevation	Meteorologically generated surge plus sea level rise

H	Total depth ($h + \zeta$)
MSL	Mean sea level at time of interest (present day or future time)
MSL_{2000s}	Present-day (2000s) MSL
SLR	Sea level rise
$SLR_{\Delta SST}$	Future projected SLR
SRF	Surge response function
SST	Sea surface temperature
U	Depth-integrated horizontal velocity
V	Wind speed
a	Constant
b	Constant
c_d	Wind drag coefficient
f	Coriolis force
h	Water depth
$h(x, y)$	Spatially variable water depth
h_o	Present-day mean water depth, and
k	Horizontal unit vector
p	Hurricane central pressure
p_o	Present-day (or historical) hurricane central pressure
p_{far}	Far-field barometric pressure
$p_{\Delta SST}$	Future projected hurricane central pressure
$p(x, y)$	Spatially variable atmospheric pressure
z	Flood elevation, relative to MSL_{2000s}
$z_{\Delta SST}$	Future flood elevation associated with ΔSST, relative to MSL_{2000s}
ΔSST	Sea surface temperature change
α	Effective earth elasticity factor
ζ	Meteorologically generated
ζ_2	Instantaneous free surface elevation
$\zeta_{\Delta SST}$	Meteorologically generated surge associated with ΔSST
η	Effective Newtonian equilibrium tide potential
ρ_a	Density of air
ρ_w	Density of water
τ_s	Wind momentum transfer into the water column, or wind stress
τ_b	Bottom shear stress

References

Ali A (1996) Vulnerability of Bangladesh to climate change and sea level rise through tropical cyclones and storm surges. J Water Air Soil Pollut 92:171–179

Ali A (1999) Impacts and adaptation assessment in Bangladesh. Clim Res 12:109–116

Blake ES, Rappaport EN, Jarrell JD et al (2006) The deadliest, costliest, and most intense United States tropical cyclones from 1851 to 2005 (and other frequently requested hurricane facts). National Weather Service NWS TPC 4

Cañizares R, Irish JL (2008) Simulation of storm-induced barrier-island morphodynamics and flooding. Coast Eng 55:1089–1101

Cayan DR, Bromirski PD, Hayhoe K et al (2008) Climate change projections of sea level extremes along the California coast. Clim Change 87:57–73

Church JA, White NJ (2006) A 20th century acceleration in global sea-level rise. Geophys Res Lett 33:L01602

Danard M, Munro A, Murty T (2003) Storm surge hazard in Canada. Nat Hazards 28:407–431

Dean RG, Bender CJ (2006) Static wave setup with emphasis on damping effects by vegetation and bottom friction. Coast Eng 53:149–156
Demernard J, Sætra Ø, Røed LP (2002) Future wind, wave and storm surge climate in the northern North Atlantic. Clim Res 23:39–49
Elsner JB, Kossin JP, Jagger TH (2008) The increasing intensity of the strongest tropical cyclones. Nature 455:92–95
Emanuel KA, Živković-Rothman M (1999) Development and evaluation of a convection scheme for use in climate models. J Atmos Sci 56:1766–1782
Emanuel KA, Sundararajan R, Williams J (2008) Hurricanes and global warming: results from downscaling IPCC AR3 simulations. Bull Am Meteorol Soc 89:347–367
Federal Emergency Management Agency (2008) Hurricane Ike storm surge. FEMA high water marks. FEMA, Washington
Gonnert G (2004) Maximum storm surge curve due to global warming for the European North Sea region during the 20th–21st century. Nat Hazard 32:211–218
Ho FP, Miller JF (1982) Pertinent meteorological and hurricane tide data for Hurricane Carla. National Oceanic and Atmospheric Administration Technical Report NWS 32, 111 pp
Holland GJ (1997) The maximum potential intensity of tropical cyclones and global climate change: a post-IPCC assessment. Bull Am Meteorol Soc 79:2519–2541
Intergovernmental Panel on Climate Change (2007) Intergovernmental Panel on Climate Change fourth assessment report. Working group 1 report: the physical science basis. http://www.ipcc.ch/ipccreports/ar4-wg1.htm. Accessed 15 August 2008
Irish JL, Cañizares R (2009) Storm-wave flow through tidal inlets and its influence on bay flooding. J Waterw Port Coast ASCE 135:52
Irish JL, Resio DT (2010) A hydrodynamics-based surge scale for hurricanes. Ocean Eng 37:69–81
Irish JL, Resio DT, Ratcliff JJ (2008a) The influence of storm size on hurricane surge. J Phys Oceanogr 38(9):2003–2013
Irish JL, Frey AE, Mousavi ME et al (2008b) Estimating the influence of projected global warming scenarios on hurricane flooding. Report prepared for the National Commission on Energy Policy (Grant No C07-00604). http://ceprofs.civil.tamu.edu/jirish/NCEPreport/index.html. Accessed 15 December 2008
Irish JL, Cialone MA, Resio DT (2009) A surge response function approach to coastal hazard assessment. Part 2: quantification of spatial attributes. Nat Hazards 51:183–205
Kirshen P, Knee K, Ruth M (2008) Climate change and coastal flooding in Metro Boston: impacts and adaptation strategies. Clim Change 90:453–473
Kleinosky LR, Yarnal B, Fisher A (2007) Vulnerability of Hampton Roads, Virginia to storm-surge flooding and sea level rise. Nat Hazards 40:43–70
Knutson TR, Tuleya RE (2004) Impact of CO_2-induced warming on simulated hurricane intensity and precipitation: sensitivity to the choice of climate model and convective parameterization. J Clim 17(18):3477–3495
Knutson TR, Tuleya RE (2008) Tropical cyclones and climate change: revisiting recent studies at GFDL. In: Dias H, Murnane R (eds) Climate extremes and society. Columbia University Press, New York
Kurihara Y, Tuleya RE, Bender MA (1998) The GFDL hurricane prediction system and its performance in the 1995 hurricane season. Mon Weather Rev 109:1629–1653
Lawrence MB, Kinberlain TB (2001) Preliminary report hurricane Bret 18–25 August 1999. National Hurricane Center Report, 10 pp
Lowe JA, Gregory JM, Flather RA (2001) Changes in the occurrence of storm surges around the United Kingdom under a future climate scenario using a dynamic storm surge model driven by the Hadley Centre climate models. Clim Dyn 18:179–188
Luettich R, Westerink JJ (2008) ADCIRC coastal circulation and storm surge model. http://www.adcirc.org. Accessed 15 December 2008
Miller L, Douglas BC (2004) Mass and volume contributions to 20th century global sea level rise. Nature 428:406–409
Mitchell JFB, Lowe J, Wood RA et al (2006) Extreme events due to human-induced climate change. Philos Trans R Soc A 364:2117–2133
Nakićenovic NJ, Alcamo G, Davis B et al (2000) Emissions scenarios: a special report of the Working Group III of the International Panel on Climate Change. Cambridge University Press, Cambridge pp 599

National Oceanic and Atmospheric Administration (1983) Pertinent meteorological data for Hurricane Allen of 1980, NOAA Technical Report NWS 35, National Oceanic and Atmospheric Administration, Silver Spring, MD
National Oceanic and Atmospheric Administration (2008a) Tides and currents. http://tidesandcurrents.noaa.gov. Accessed 15 December 2008
National Oceanic and Atmospheric Administration (2008b) Historical hurricane tracks. http://maps.csc.noaa.gov/hurricanes/index.jsp. Accessed 15 December 2008
National Weather Service (2000) Hurricane history. http://www.srh.noaa.gov/crp/docs/research/hurrhistory/. Accessed 15 December 2008
Otto-Bliesner BL, Marshall SJ, Overpeck JT et al (2006) Simulating Arctic climate warmth and icefield retreat in the last interglaciation. Science 311:1751–1753
Pan H-L, Wu W-S (1995) Implementing a mass flux convection parameterization package for the NMC medium-range forecast model. NMC Office Note 409
Pfeffer WT, Harper JT, O'Neel S (2008) Kinematic constraints on glacier contributions to 21st-century sea-level-rise. Science 321:1340–1343
Rahmstorf S (2007) A semi-empirical approach to projecting future sea-level rise. Science 315:368–370
Rohling EJ, Grant K, Hemleben C et al (2008) High rates of sea-level rise during the last interglacial period. Nature Geoscience 1:38–42
Simpson RH (1974) The hurricane disaster-potential scale. Weatherwise 27:169 and 186
Thompson EF, Cardone VJ (1996) Practical modeling of hurricane surface wind fields. J Waterw Port C ASCE 122:195–205
Travis J (2005) Hurricane Katrina: scientists' fears come true as hurricane floods New Orleans. Science 309:1656–1659
United States Geological Survey (2008) National Elevation Dataset. http://ned.usgs.gov/. Accessed 15 December 2008
US Army Corps of Engineers (1968) Report on Hurricane Beulah 8–21 September 1967. US Army Corps of Engineers Galveston District Report,pp 143
US Army Corps of Engineers (2006) Performance evaluation of the New Orleans and southeast Louisiana hurricane protection system draft final report of the Interagency Performance Evaluation Task Force. US Army Corps of Engineers Report, pp 259
Vecchi GA, Soden BJ (2007) Effect of remote sea surface temperature change on tropical cyclones potential intensity. Nature 450:1066–1070
Vickery PJ, Skerlj PF, Steckley AC et al (2000) Hurricane wind field model for use in hurricane simulations. J Struct Eng ASCE 126:1203–1222
Webster PJ, Holland GJ, Curry JA et al (2005) Changes in tropical cyclone number, duration, and intensity in a warming environment. Science 309:1844–1846
White NJ, Church JA, Gregory JM (2005) Coastal and global averaged sea-level rise for 1950 to 2000. Geophys Res Lett 32:L01601
Wigley TML (2004) Magicc/Scengen. http://www.cgd.ucar.edu/cas/wigley/magicc/. Accessed 15 December 2008